Iron-Mediated Amination of Hydrocarbons in the Gas Phase

by **Mark Brönstrup**, **Ilona Kretzschmar**, **Detlef Schröder**, and **Helmut Schwarz***

Institut für Organische Chemie der Technischen Universität Berlin, Straße des 17. Juni 135, D-10623 Berlin

Dedicated to Professor *Werner Schroth* on the occasion of his 70th birthday

$FeNH^+$ is chosen as a model system to probe the transition-metal-mediated transfer of imine groups in the gas phase by mass-spectrometric means. *Ab initio* calculations at the MR-ACPF level predict $FeNH^+$ to have a linear sextet ground state ($^6\Sigma^+$); a bent quartet state ($^4A'$) and a linear doublet state ($^2\Delta$) are higher in energy by 0.14 eV and 0.51 eV, respectively. The bond-dissociation energy is determined to $D(Fe^+-NH) = 69 \pm 2$ kcal mol^{-1} using ion-molecule reactions. Charge-stripping experiments combined with *ab initio* calculations yield an ionization energy of $IE(FeNH^+) = 15.7 \pm 0.5$ eV. The chemical behavior of $FeNH^+$ towards oxygen, water, hydrogen, aliphatic hydrocarbons, benzene, and toluene reveals an intrinsically high reactivity of $FeNH^+$. Because a transfer of the $\langle NH \rangle$ fragment to the substrate is feasible in most cases, attractive amination reactions like methane → methylamine, benzene → aniline, or toluene → benzylidenamine can be afforded by $FeNH^+$.

Introduction. – The task to introduce an amino function into organic molecules has been solved by a variety of chemical transformations [1]. Probably, the simplest and most direct access to $R-NH_2$ units involves the insertion of the imine fragment $\langle NH \rangle$ in a C–H bond of the substrate according to *Reaction 1*.

$$R-H + \langle NH \rangle \longrightarrow R-NH_2 \quad (1)$$

Naked imine is an energy-rich compound ($\Delta H_f = 90$ kcal mol^{-1}), and its usually endothermic formation requires high temperatures [2]. To circumvent harsh conditions, procedures for reacting NH equivalents with hydrocarbons have to be applied. For practical purposes, this is often accomplished by a combination of an oxidation step (*e.g.*, hydroxylation or chlorination) followed by nucleophilic substitution with a nitrogen base (*e.g.*, ammonia). More promising approaches would, however, involve transition metals which may serve to generate and bind the imine fragment, and eventually to transfer it to the organic substrate. In the condensed phase, a large number of transition-metal-imido complexes [M]NH are known [3] that undergo an intriguing variety of chemical reactions. Depending on the electronic environment provided by [M], the character of the imine ligand can be tuned from nucleophilic [4] to electrophilic [5]. Among the reactions observed are *Wittig*-type reactions [6], NH addition to olefins [7], cycloadditions [4b][8], and even activations of aliphatic and aromatic C–H bonds [9]. According to theoretical studies [10], the electrophilic character of the imine unit increases upon moving [M] from the bottom left to the upper right in the periodic table. In contrast to an extensive research activity in the condensed phase, only few studies have addressed the intrinsic structural properties and the reactivity of ionic $[M]NH^{+/-}$ species in the gas phase [11–15]. In analogy to the

reactivity of the isolobal metal-oxide cations MO^+ towards H_2O in the gas phase [16], the M^+-NH bond dissociation energies (D) of early transition-metal imines (M = Sc, Ti, V, Y, Zr, Nb, La, Ta) are large enough to promote dehydrogenation of ammonia [11], *i.e.*, $D(M^+-NH) > 101$ kcal mol^{-1}. A direct and unfortunate consequence of these high bond energies is, however, that the MNH^+ cations of the early transition metals are featured by a low reactivity as far as transfer of the imine unit to a substrate is concerned. The late 3d-transition-metal cations Co^+, Ni^+, and Cu^+ differ in that even at elevated kinetic energies, they do not form the corresponding metal-imine cations when reacted with NH_3 [17].

This contribution is focused on iron, because $FeNH^+$ is expected to possess a well-balanced bonding situation between these extremes along the 3d series, rendering it a suitable candidate for catalytic procedures. In fact, *Freiser* and coworkers have demonstrated, in a pioneering study about transition-metal imines, that in the gas phase $FeNH^+$ is able to transfer the imine unit to benzene and ethene [13]. Here, we report some spectroscopic properties of $FeNH^+$ derived from a combination of mass-spectrometric experiments with high-level *ab initio* calculations, and examine the chemical behavior of $FeNH^+$ towards a series of small organic and inorganic substrates experimentally.

Experimental and Computational Details. – Most experiments were performed with a *Spectrospin CMS 47X* FTICR mass spectrometer which has been described in detail before [18][19]. Briefly, Fe^+ ions were generated *via* laser desorption/laser ionization by focusing the beam of a Nd : YAG laser (*Spectron Systems*, $\lambda =$ 1064 nm) onto an iron target. The ions are extracted from the source and transferred into the analyzer cell by a system of electrostatic potentials and lenses. After deceleration, the ions are trapped in the field of a superconducting magnet (maximum field strength 7.05 T). Prior to ion/molecule reactions, the $^{56}Fe^+$ isotope was mass-selected by using the FERETS technique [20]. $FeNH^+$ was generated by two different procedures. *i*) $^{56}Fe^+$ was converted into $FeNH^+$ (turnover *ca.* 50%) by pulsing-in a mixture of Ar and HN_3 (Ar/HN_3 *ca.* 1000 : 1). *ii*) After complete conversion of $^{56}Fe^+$ into FeO^+ by pulsed-in N_2O, FeO^+ was reacted with leaked-in NH_3 ($p = 4 \cdot 10^{-9}$ mbar) to yield $FeNH^+$ within 3 s. $FeNH^+$ was isolated using FERETS and subsequently reacted with the neutral reactant, which was leaked-in continuously at $p = 5 - 200 \cdot 10^{-9}$ mbar. Both methods of $FeNH^+$ generation were applied for each neutral reagent. Data were accumulated and processed by means of an *ASPECT 3000* minicomputer. The elemental composition of product ions was verified by high-resolution experiments ($m/\Delta m > 100\,000$) that allowed for a clear distinction of ions with equal nominal masses, *e.g.*, $FeNH_2^+$ and FeO^+. Analysis of the pseudo-first-order kinetics of the ion/molecule reactions provides branching ratios and effective bimolecular rate constants k which are reported within experimental errors of ± 10% and ± 50%, resp. Secondary reactions were either too slow to be observed within the time frame of the experiment or consisted of association processes, which are not further considered in the present study.

All experiments concerning $FeNH^+$ dications were performed with a modified *VG/ZAB/HF/AMD* four-sector mass spectrometer of *BEBE* configuration (*B* stands for magnetic and *E* for electric sector), which has been described in detail in [21]. Briefly, $Fe(CO)_5$ was admitted to the ion source *via* the heated septum inlet system, and HN_3 was introduced *via* the metal-free glass/*Teflon* inlet system. The mixture was ionized by a beam of electrons (100 eV) in a chemical ionization source (repeller voltage *ca.* 0 V). For collisional activation (CA) spectra, the ions of interest were mass-selected by means of $B(1)/E(1)$ at a resolution of $m/\Delta m = 3000$ and collided with He (80% transmission) in the field-free region preceding $B(2)$. The fragmentations were recorded by scanning $B(2)$. Energy-resolved charge-stripping (CS) spectra [22] were recorded by using the first two sectors, owing to the higher energy resolution of $E(1)$ compared to $B(2)$. To this end, $FeNH^+$ was mass-selected *via* $B(1)$, collided with O_2 (60% transmission), and the resulting species were recorded by scanning $E(1)$. The high-energy onsets of $FeNH^+$ and $FeNH^{2+}$ were compared with each other and converted to absolute energy differences. For calibration of the energy scales by a multiplicative correction method, the well-known process $C_7H_8^+ \rightarrow C_7H_8^{2+}$ ($Q_{min} = 15.7$ eV) was used [23].

HN_3 was prepared by dropping conc. H_2SO_4 into a soln. of NaN_3 in H_2O; aq. HN_3 solns. containing up to 20% HN_3 can be handled safely [24]. To minimize the transfer of H_2O from the HN_3 stock soln. to the gas

reservoir of the ICR pulse valve, the soln. was frozen with liquid N_2, evacuated, thawed to no more than 0°, and then connected to the gas reservoir for *ca.* 0.1 s. Other neutral gaseous reagents were commercially available and used without further purification (purities: $NH_3 > 99.98\%$; $O_2 > 99.995\%$; $H_2 > 99.999\%$; $CH_4 > 99.95\%$; C_2H_6, C_3H_8, C_4H_{10}, and i-$C_4H_{10} > 99.5\%$). Liquids were purified by gas chromatography and had a purity > 99%.

Full geometry optimizations were performed at the B3LYP level of theory [25] with a 6-311 + G* basis set for all atoms as implemented in GAUSSIAN 94 [26]. The obtained minima were verified by frequency calculations. Single-point energies were calculated with the MOLPRO 96 program package [27] at the multi reference-average coupled pair functional (MR-ACPF) level [28] using the following atomic natural orbital (ANO) basis sets. Fe: (21s 15p 10d 6f 4g)/[8s 7p 5d 3f 2g]; N: (14s 9p 4d 3f)/[6s 5p 3d 2f]; H: (8s 4p 3d)/[4s 3p 2d] [29][30]. The active space included the 3d and 4s orbitals of Fe, the 2s and 2p orbitals of N, and the 1s orbital of H. To test the reliability of the applied procedure, the bond dissociation energy of FeO^+ ($^6\Sigma^+$) was calculated at the same level. A value of 78 kcal mol^{-1} was obtained, in good agreement with the well-established experimental value of 80.1 kcal mol^{-1} [31].

Results and Discussion. – The paper is organized such that we will first describe the reactions which can be used to generate $FeNH^+$. Then, the electronic and thermochemical properties of $FeNH^+$ are evaluated by experimental and theoretical means, *inter alia* leading to a bracketing of the Fe^+-NH bond energy. The knowledge of these properties is used in the interpretation of the chemical reactions of $FeNH^+$ with a series of simple inorganic and organic substrates.

Generation of FeNH+. In the gas phase, the $FeNH^+$ cation can be generated from simple precursors *via* three different pathways according to *Reactions 2–4*[1]).

$$FeO^+ + NH_3 \longrightarrow FeNH^+ + H_2O \quad 85\% \quad (2a)$$

$$FeO^+ + NH_3 \longrightarrow FeOH^+ + NH_2^{\bullet} \quad 15\% \quad (2b)$$

$$Fe^+ + HN_3 \longrightarrow FeNH^+ + N_2 \quad 70\% \quad (3)$$

$$Fe^+ + NH_2OH \longrightarrow FeNH^+ + H_2O \quad \approx 20\% \quad (4)$$

The reaction of FeO^+ with NH_3 proceeds fast ($k = 8.3 \cdot 10^{-10}$ cm^3 molecules^{-1} s^{-1}). However, more instructive than comparing mere rate constants is the comparison of the measured rate constants with the respective gas kinetic collision rate constants k_c [33]. For *Reaction 2*, k_c is $21.7 \cdot 10^{-10}$ cm^3 molecules^{-1} s^{-1}; thus, the reaction efficiency, defined as $\phi = k/k_c$, amounts to *ca.* 0.4 for *Reaction 2*. The formation of $FeNH^+$ *via Reaction 2a* is the predominating channel and has been reported previously [13], whereas the side *Reaction 2b* to yield the $FeOH^+$ cation has not been mentioned before. The required FeO^+ precursor is most conveniently generated in one of the two following reactions [34].

$$Fe^+ + N_2O \longrightarrow FeO^+ + N_2 \quad 100\% \quad (5)$$

$$Fe(CO)^+ + O_2 \longrightarrow FeO^+ + CO_2 \quad 100\% \quad (6)$$

The combined yield of $FeNH^+$ obtained *via Reactions 2* and *5* is satisfactory (up to 80%), because *i*) *Reaction 2* is fast as compared to *Reaction 5* [34b], *ii*) FeO^+ does not

[1]) For the generation of metal imines using isocyanates, see [32].

react with N_2O, and *iii*) clustering of $FeNH^+$ with NH_3 is inefficient under the experimental conditions chosen. Unfortunately, however, in a pulsed operation of the ICR spectrometer, NH_3 cannot be completely pumped-off from the reaction cell during the duty cycle. Therefore, *Reaction 2* is not suited for monitoring the reactions of $FeNH^+$ with those substrates for which the rate constants are rather small, and cases where the primary reaction products undergo fast consecutive reactions (*e.g.*, ligand exchange) with NH_3. Further, the generation of $FeNH^+$ *via Reaction 2* by chemical ionization of a $Fe(CO)_5/N_2O/NH_3$ mixture is not practical due to non-avoidable isobaric interferences, *e.g.*, $^{56}FeNH^+$ and $^{54}FeOH^+$ (both 71 amu).

Reaction 3 represents the isoelectronic analog of *Reaction 5* for the generation of FeO^+. Interestingly, NH transfer *via Reaction 3* proceeds gently and with a significantly larger efficiency than oxygen transfer *via* reaction (5), *i.e.*, $\phi(3) \geq 0.4$ *vs.* $\phi(5) = 0.06$. Preliminary data also indicate that this reaction is not restricted to iron, but can be applied for a broad range of transition-metal cations[2]). This versatility of HN_3 as an imine precursor can be attributed to its property as a high-energy material, and formation of N_2 constitutes the driving force of the reaction, *i.e.*, liberation of NH from HN_3 requires only 21 kcal/mol. The reaction of gaseous HN_3 with Fe^+ ions gives good yields of $FeNH^+$ (70%). However, $FeNH^+$ continues to react with HN_3 to yield predominately Fe^+ (50%) and FeH^+ (25%) along with several side products with an overall rate constant of *ca.* $2.5 \cdot 10^{-10}$ cm^3 molecules^{-1} s^{-1}; hence, unlike *Reaction 5* no complete conversion $Fe^+ \rightarrow FeNH^+$ can be achieved. Surprisingly, the pumping characteristics of gaseous HN_3 are superior to those of NH_3, and HN_3 can be introduced to the ICR also *via* pulsed valves. Further, isobaric interferences are negligible in chemical ionization of $Fe(CO)_5/HN_3$ which is suited for generation of $FeNH^+$.

Reaction 4 appears as a straightforward route to generate $FeNH^+$; however, the yields obtained are moderate (20%), and considerable amounts of $FeOH^+$ (40%), FeO^+ (25%), and higher association products (15%) are formed in competition to *Reaction 4*. Moreover, the storage of NH_2OH in the metal-containing inlet systems and reservoirs is accompanied by significant decomposition. Thus, this route is not practical for the generation of $FeNH^+$. Due to uncertainties with respect to the actual composition of the gaseous phase, we also refrain from reporting rate constants for the reactions of NH_2OH. In summary, only *Reactions 2* and *3* were used for the generation of $FeNH^+$ in all experiments.

Spectroscopic Properties of FeNH$^+$. A central topic regarding the electronic features of $FeNH^+$ concerns the spin multiplicity of the molecule. For related species in organometallic gas-phase chemistry, spin multiplicity has been demonstrated to be a crucial, decisive factor for chemical reactivity [35]. The NH fragment is isolobal to O and CH_2, and, hence, $FeNH^+$ can be compared to FeO^+, which possesses a sextet ground state ($^6\Sigma^+$) [36], and to $FeCH_2^+$, for which the $^4B_2$ quartet state was found to be lowest in energy [37].

---

[2]) Exceptions are Mn^+, Ag^+, and Cd^+, which are completely unreactive due to their electronic features. Thermalized Cr^+ is also unreactive; however, after electronic excitation, partial conversion to $CrNH^+$ was achieved. For oxophilic metals like Zr^+, Hf^+, Nb^+, Ta^+, or W^+, the obtained yields of MNH^+ are low due to the preferred formation of oxides with background H_2O and formation of metal nitrides.

One should be aware of the fact that a reliable theoretical treatment of coordinatively unsaturated transition-metal compounds, like $FeNH^+$, still constitutes a challenge even for state of the art quantum-chemical calculations[3]). As a reasonable compromise, we optimized the geometries with the B3LYP approach and then calculated the energies of stationary points at the MR-ACPF level of theory starting from the corresponding complete active space self-consistent field (CASSCF) wave functions.

According to these calculations, $FeNH^+$ possesses a $^6\Sigma^+$ sextet ground state, and the bond dissociation energy of $FeNH^+$ ($^6\Sigma^+$) to yield Fe^+ (^6D) and NH ($^3\Sigma^-$) ground states is predicted as 57.9 kcal mol^{-1} including ZPVE (*Table 1*). Interestingly, the lowest-lying quartet state $FeNH^+$ ($^4A'$) is only 0.14 eV higher in energy than $FeNH^+$ ($^6\Sigma^+$), and even excitation to the doublet state $FeNH^+$ ($^2\Delta$) requires no more than 0.51 eV. This rather small gap between the ground state and the first excited electronic states might as well have been deduced from a comparison of the FeX^+ compounds of the isolobal fragments $X = CH_2$, NH, and O. The iron/group 14 compound $FeCH_2^+$ has a $^4B_2$ quartet ground state with excitation energies of only *ca.* 0.25–0.4 eV to the $^6A_1$ and $^6B_1$ sextet states [39], and 1.4–1.6 eV to the almost degenerate $^2A_1$ and $^2A_2$ doublet states [37]. Instead, a detailed *ab initio* study [36] predicts a $^6\Sigma^+$ ground state for FeO^+ (the iron/group 16 compound) with an excitation energy of *ca.* 0.5–0.8 eV to the quartet state FeO^+ ($^4\Phi$). Consequently, $FeNH^+$ containing the group 15 fragment NH is expected to be featured by a close energetic proximity of the different spin states as indeed predicted by the *ab initio* results. With respect to chemical reactivity, the narrow state splittings suggest that spin changes may be quite facile in the reactions of $FeNH^+$. Hence, the 'two-state-reactivity' (TSR) concept [35] has to be applied for an accurate description of the chemical behavior of this cation. The TSR concept explicitely acknowledges spin-orbit-coupling-mediated crossovers between surfaces of different spin multiplicity during the course of a reaction.

The influence of electron spin on the minimum geometry of $FeNH^+$ becomes obvious by considering the significantly different Fe–N–H angles. The sextet and the doublet states exhibit linear Fe–N–H arrangements (*Fig. 1*), while the quartet state is bent (141°) at its minimum. However, the MR-ACPF calculations demonstrate that the potential-energy surfaces are smooth with respect to the bending mode. For example, bending of $FeNH^+$ ($^6\Sigma^+$) to 140° requires an energy of only 3.4 kcal mol^{-1}, and linear $FeNH^+$ ($^4A'$) is only 2.0 kcal mol^{-1} higher in energy than its bent minimum (*Fig. 1*). The corresponding harmonic stretching frequencies are 327 cm^{-1} ($^6\Sigma^+$), 387 cm^{-1} ($^4A'$), and 401 cm^{-1} ($^2\Delta$). The Fe–N bond lengths of the energetic minima are very similar for all spin states, *i.e.*, 1.725 Å for $FeNH^+$ ($^6\Sigma^+$) *vs.* 1.731 Å for $FeNH^+$ ($^4A'$), and 1.713 Å for $FeNH^+$ ($^2\Delta$). The dependences of the Fe–N bond lengths on the Fe–N–H angles are displayed in *Fig. 2*. Whereas changes are negligible for $FeNH^+$ ($^2\Delta$), bending of the Fe–N–H unit leads to a considerable elongation of the Fe–N bonds for $FeNH^+$ ($^6\Sigma^+$) and even more so for $FeNH^+$ ($^4A'$). This parallels the simplistic valence-bond picture of a triple bond from the metal to the sp-hybridized N-atom for a linear M–N–H

---

[3]) A high-level *ab initio* study of neutral FeN, which is equivalent to deprotonated $FeNH^+$, can be found in [38].

Table 1. *Optimized Geometries* (bond lengths in Å and angles in degree) *and Total Energies* (Hartree)[a]) *of Different Electronic States of $FeNH^+$ and $FeNH^{2+}$ at the ACPF Level of Theory Using the B3LYP-Optimized Geometries of the Different States.* In addition, some relevant fragment energies are given.

	State	r(Fe–N)	r(N–H(2))	α(FeNH)	ACPF	ZPVE [eV]	E_{rel}[b]) [eV]
$FeNH^+$	$^6\Sigma^+$	1.725	1.020	180	– 1317.62233	0.30	0.00
	$^4A'$	1.731	1.026	141	– 1317.61659	0.28	0.14
	$^2\Delta$	1.713	1.028		– 1317.60243	0.27	0.51
$FeNH^{2+}$	$^7\Sigma^-$	2.096	1.043	180	– 1317.05999	0.29	15.29
		1.725	1.020	180	– 1317.01205		16.60[c])
	$^5\Delta$	1.852	1.047	180	– 1317.05909	0.29	15.32
		1.725	1.020	180	– 1317.03977		15.84[c])
	$^3\Sigma^-$	1.916	1.049	180	– 1317.05202	0.29	15.51
		1.725	1.020	180	– 1317.05271		15.49[c])[d])
Fe^+	^{6}D				– 1262.37536		
NH	$^3\Sigma^-$		1.042		– 55.15097	0.20	
Fe^{2+}[e])	$^6A_2$				– 1261.79650		
NH^+[e])	$^2\Pi$		1.047		– 54.65921	0.19	

[a]) 1 Hartree = 627.51 kcal mol^{-1}. [b]) ZPVE is included. [c]) Energy of the dication state at the equilibrium geometry of the $FeNH^+$ ($^6\Sigma^+$) monocation ground state. Accordingly, these entries correspond to the vertical ionization energies of the monocation. [d]) Note that ACPF predicts the triplet state of the dication having the geometry of $FeNH^+$ ($^6\Sigma^+$) to be slightly more stable than the B3LYP-optimized $FeNH^{2+}$ ($^3\Sigma^-$) structure, demonstrating the limitations of the combined ACPF//B3LYP approach. [e]) As expected, the calculated $IE(Fe^+) = 15.75$ and $IE(NH) = 13.38$ eV are slightly underestimated at this level of theory as compared to the experimental data, *i.e.*, $IE(Fe^+) = 16.18$ and $IE(NH) = 13.49$ eV [41].

arrangement and a (longer) double bond to the sp^2-hybridized N-atom in a bent M–N–H geometry. However, due to the contribution of at least eight different resonance structures to the metal–imine bond [10b], a simple correlation between the bond order and the degree of bending does not exist [3][4a][10a][40]. According to *Cundari*, the metal–imine bond order generally lies between two and three [10b]. In the condensed-phase chemistry of bent and linear transition metal-imido complexes, steric demands and electronic effects of R and co-ligands are regarded as the determining factors for the MNR bond angles. The present calculations on 'naked' $FeNH^+$, that serves as a model system which is unperturbed by any ligand effects or steric hindrance, demonstrate that the discussion of metal–imine geometries must also acknowledge the actual spin multiplicities. In particular, the weak bending forces add a note of caution towards a generalization of trends in bond lengths and angles, in that these soft potentials may be determined by rather subtle effects, *e.g.*, counterions or packing.

An experimental estimate of the Fe^+–NH bond energy can be obtained by the bracketing technique. As thermalized ions undergo only almost thermoneutral or exothermic reactions under the low-pressure conditions prevailing in an ICR spectrometer ($p \approx 10^{-9}$–10^{-6} mbar), the occurrence of the following two reactions allows an approximate determination of the lower and upper limits of $D(Fe^+–NH)$ [31][41].

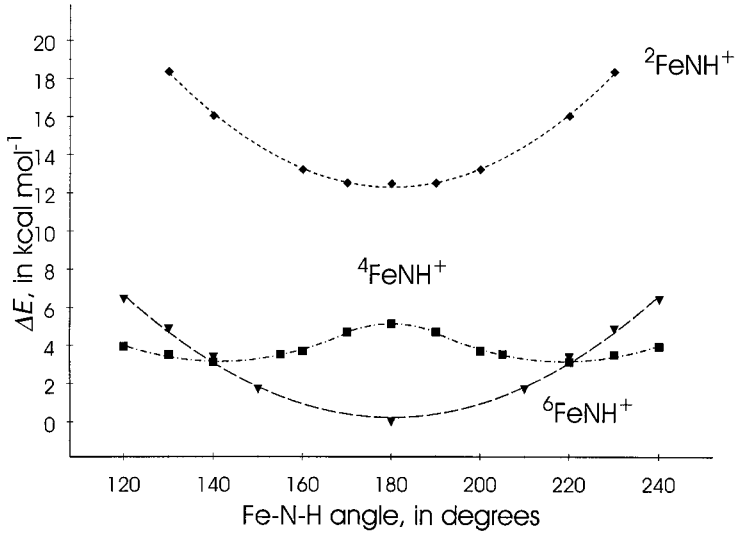

Fig. 1. *Energy dependence of $^6FeNH^+$, $^4FeNH^+$, and $^2FeNH^+$ on the Fe–N–H angle.* Total energies are obtained from single-point calculations at the MR-ACPF level using the B3LYP-optimized structures (see text) and are given in kcal mol^{-1} relative to linear $^6FeNH^+$.

$$FeO^+ + NH_3 \longrightarrow FeNH^+ + H_2O \quad \Rightarrow D(Fe^+{-}NH) > 63.6 \pm 1.4 \text{ kcal mol}^{-1} \quad (2a)$$

$$FeNH^+ + CH_4 \longrightarrow Fe^+ + CH_3NH_2 \quad \Rightarrow D(Fe^+{-}NH) < 77.7 \pm 0.5 \text{ kcal mol}^{-1} \quad (7)$$

Interestingly, when mass-selected $FeNH^+$ is reacted with H_2O ($p_{H_2O} \approx 10^{-7}$ mbar) in the absence of NH_3, a small, but clearly detectable amount of FeO^+ is formed. To ensure that the formation of cationic iron oxide corresponds to a genuine reaction of $FeNH^+$ with H_2O rather than to reactions with possible background contaminants, also the reaction of $FeNH^+$ with $H_2{}^{18}O$ was examined while continuously ejecting $Fe^{16}O^+$; formation of $Fe^{18}O^+$ from the $FeNH^+/H_2{}^{18}O$ couple unambiguously establishes the occurrence of the reversal of *Reaction 2a*. Nevertheless, the reverse reaction to yield FeO^+ is rather slow, and the rate constant is *ca.* 4500 ± 1500 times lower than that of the forward reaction. While side reactions as well as association processes prevent to establish an equilibrium between $FeNH^+$ and FeO^+ in the presence of NH_3 and H_2O (see below), the ratio of the forward and backward reaction rate constants (k_f/k_b) can be used to derive a refined bracket by using the *Gibbs-Helmholtz* equation, $k_f/k_b = K_{eq} = \exp(-\Delta_R G/RT)$. Assuming that the ions react at room temperature [34a][42], and that the reactions proceed without barriers in excess of the respective thermochemical thresholds, we arrive at $\Delta_R G(298) = -5.0 \pm 0.7$ kcal mol^{-1} for *Reaction 2a*. The assumption that forward and backward reactions are barrierless with respect to the entrance channels appears justified because *i*) *Reaction 2a* occurs with a reasonable efficiency, and *ii*) it may occur in a sequence of formal proton-transfer steps which are often quite facile [43]. Further, B3LYP calculations reveal that thermal contributions to *Reaction 2a* can be neglected (*ca.* 0.1 kcal mol^{-1}); therefore, we set $\Delta_R G(298) \cong \Delta H_r(298)$. Accordingly, we arrive at $D(Fe^+{-}NH) = 69 \pm 2$ kcal mol^{-1},

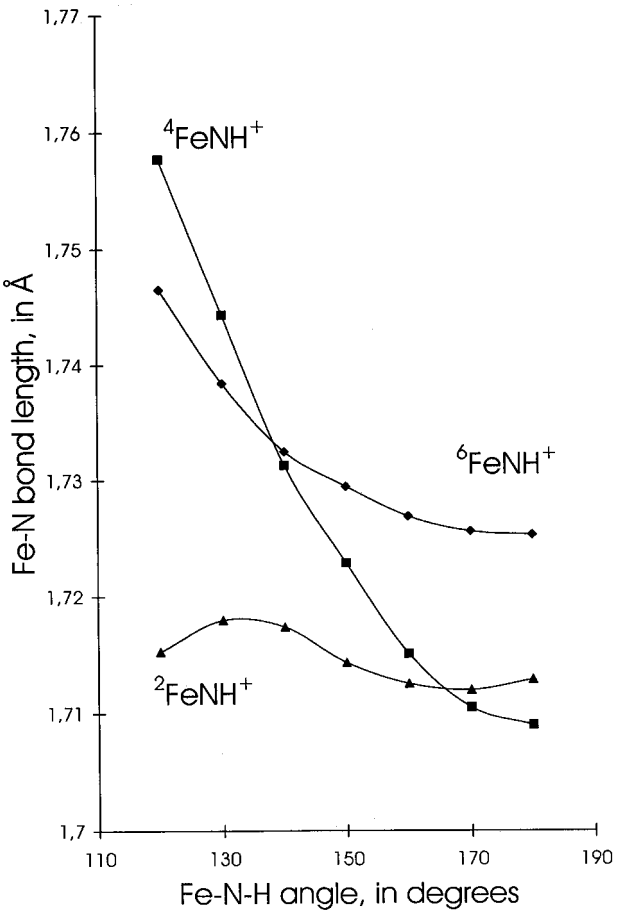

Fig. 2. *Dependence of the Fe–N bond length on the Fe–N–H angle for* $^6FeNH^+$, $^4FeNH^+$, *and* $^2FeNH^+$. Structures are optimized at the B3LYP level with fixed angles.

which agrees well with an earlier experimental value of 75 ± 11 kcal mol^{-1} derived by an analogous ICR bracketing experiment[4]). Slightly lower values, but close to the error margins, are $D(Fe^+-NH) = 61 \pm 5$ kcal mol^{-1} as determined by photodissociation [13][14], and the theoretical value $D(Fe^+-NH) = 57.9$ kcal mol^{-1} derived in this work. Interestingly, the group 15 fragment NH is bound much weaker to Fe^+ than the related fragments CH_2 ($D(Fe^+-CH_2) = 81.5 \pm 0.9$ kcal mol^{-1}) [45] and O ($D(Fe^+-O) = 80.1 \pm 1.4$ kcal mol^{-1}) [31] which nicely correlates with the thermochemistry of the free fragments, *e.g.*, $D(H_2C-CH_2) = 174$ kcal mol^{-1}, $D(H_2C-NH) = 151$ kcal mol^{-1}, and $D(CH_2-O) = 178$ kcal mol^{-1}.

---

[4]) In our evaluation, the bracketed value $D(Fe^+-NH) = 54 \pm 14$ kcal mol^{-1} reported earlier in [13] was updated for the most recent thermochemical data of the participating species and also corrected for some arithmetical errors in the calculation of the bracket.

The existence of neutral FeNH is revealed by neutralization/reionization (NR) [46] experiments in a sector-field mass spectrometer. Thus, cationic $FeNH^+$ was neutralized with Xe as a collision gas, and after removal of all ionic species, the fast-moving beam of neutrals was reionized by collision with O_2, subsequently mass-analyzed and detected. Next to signals for Fe^+ (100%) and $FeNH^+$ (8%), the NR spectrum is featured by a survivor signal for $FeNH^+$ (25%), demonstrating that neutral FeNH is stable on the μs time scale. Unfortunately, however, an unambiguous determination of the first ionization energy of FeNH by bracketing experiments was not feasible, because $FeNH^+$ turned out to undergo fast chemical reactions that compete efficiently with electron transfer with all investigated substrates which have ionization energies in the desired range below 9 eV, *e.g.*, substituted arenes (see below). An upper limit of $IE(FeNH) \leq 8.4 \pm 0.3$ eV can be derived from the occurrence of inefficient charge transfer to mesitylene ($IE = 8.41$ eV[5]).

The properties of the $FeNH^+$ dication were investigated by a charge-stripping experiment [23], in which mass-selected $FeNH^+$ was collided with O_2 as a target gas. Next to fragmentation products of the monocation, *i.e.*, Fe^+ (100%), FeN^+ (80%), FeH^+ (6%), NH^+ (0.1%), and N^+ (0.1%), some dications were observed, *i.e.*, $FeNH^{2+}$ (4%) and Fe^{2+} (1%). Furthermore, the $FeNH^{2+}$ dication generated in the ion source from $Fe(CO)_5/HN_3$, was mass-selected and collided with He, yielding $FeNH^+$ (50%), FeN^+ (40%), and Fe^+ (100%) as single charged and Fe^{2+} (60%) as doubly charged fragments. The Fe^+ channel has a composite peak shape which is characteristic for a competition of *i*) consecutive fragmentation of $FeNH^+$ monocation formed by charge exchange with He and *ii*) *Coulomb* explosion to yield Fe^+ and NH^+; the latter monocation is not observed, however. The ionization energy of $FeNH^+$, *i.e.*, the second ionization energy of FeNH, has been determined quantitatively by energy-resolved charge-stripping experiments [22]. The energy required for the ionization of $FeNH^+$ to yield $FeNH^{2+}$ is provided by the kinetic energy of the projectile cation in the collision with the target. If one assumes that ionization occurs from the electronic ground state, the minimum loss of kinetic energy (Q_{min}) corresponds to the vertical ionization energy (IE_v) of the projectile[6]). Experimentally, the translational energy loss determined by charge stripping leads to $IE_v(FeNH^+) \approx Q_{min} = 16.3 \pm 0.4$ eV[7]).

The ACPF level of theory suggests three low-lying states for $FeNH^{2+}$ dication on the triplet, quintet, and septet surfaces (*Table 1*). Indeed, the splitting of these states is narrow (within 0.2 eV), and the accuracy of the computational approach used does not permit a definite assignment of the ground state for the dication. Interestingly, the vertical ionization energies with respect to $FeNH^+$ ($^6\Sigma^+$) are more divergent. Thus, almost identical energies are required for the vertical and adiabatic ionizations $FeNH^+(^6\Sigma^+) \rightarrow FeNH^{2+}(^3\Sigma^-)$, while the vertical ionizations to $FeNH^{2+}$ ($^5\Delta$) and $FeNH^{2+}(^7\Sigma^-)$ are by 0.5 and 1.3 eV, respectively, more energy demanding than

---

5) The reaction proceeds with maximum efficiency ($\phi = 1$) and mainly yields dehydrogenation analogous to the $FeNH^+$/toluene couple (see text). Charge-transfer products account for less than 3% of the overall products.

6) According to the *Franck-Condon* principle, ionization proceeds much faster than the motion of the nuclei; therefore, Q_{min} corresponds to the vertical ionization energy.

7) Three independent measurements with O_2 as target gas (70% transmission) gave $Q_{min} = 16.07$ eV, 16.43 eV, and 16.29 eV.

the corresponding adiabatic processes. Therefore, one might anticipate that the threshold for dication formation measured in the charge-stripping experiment would coincide with the formation of $FeNH^{2+}$ ($^3\Sigma^-$) and thus predicting $IE_v(FeNH^+ (^6\Sigma^+)) = 15.5$ eV. However, simple electron-counting rules reveal that the transition $FeNH^+(^6\Sigma^+) \rightarrow FeNH^{2+}(^3\Sigma^-)$ cannot proceed as a vertical process, because, in addition to the removal of one electron, it requires spin-coupling of two electrons in order to reach the triplet dication starting from the sextet precursor[8]). Similarly, $FeNH^+$ ($^4A'$) cannot yield $FeNH^{2+}$ ($^3\Sigma^-$) by a one-electron removal, because $FeNH^+$ ($^4A'$) transforms to a $\delta^1\pi^1\sigma^1$ configuration of unpaired electrons in a linear arrangement while the $FeNH^{2+}$ ($^3\Sigma^-$) dication state has a $\delta^2\pi^0\sigma^0$ occupation. Instead, we suggest that the Q_{min} value determined experimentally corresponds to ionization to the $FeNH^{2+}$ ($^5\Delta$) and $FeNH^{2+}$ ($^7\Sigma^-$) states. Following this line of reasoning, theory suggest a threshold of $IE_v = 15.84$ eV for dication formation associated with the transition $FeNH^+$ ($^6\Sigma^+$) $\rightarrow FeNH^{2+}(^5\Delta)$. This value is in pleasingly good agreement with the measured Q_{min} value of 16.3 ± 0.4 eV. The minor discrepancy between these results follows the close analogy of the experimental and calculated values for $IE(Fe^+)$, *i.e.*, 16.18 and 15.85 eV, respectively. We note in passing that the underestimation of experimental *IE*s is a general trend expected at this level of theory which can be attributed to the limited treatment of correlation energy. Combining the experimental and theoretical data, the adiabatic ionization energy (IE_a) involving the respective ground states, *i.e.*, the transition $FeNH^+$ ($^6\Sigma^+$) $\rightarrow FeNH^{2+}$ ($^7\Sigma^-$), is predicted as $IE_a = 15.7 \pm 0.5$ eV[9]). Again, the minor underestimation of the calculated $IE_a = 15.3$ eV is quite expected at this level of theory.

In combination with the bracketed value for $D(Fe^+-NH)$ and additional thermochemical data, the knowledge of $IE(FeNH^+)$ allows to evaluate the thermochemical stability of $FeNH^{2+}$ dication in terms of a thermochemical cycle. Thus, the energy required for the dissociation of $FeNH^{2+}$ into Fe^{2+} and NH is predicted as $D(Fe^{2+}-NH) = 80 \pm 14$ kcal mol^{-1}. Moreover, also the *Coulomb* explosion into Fe^+ and NH^+ is predicted to be endothermic by 18 ± 14 kcal mol^{-1}. Accordingly, $FeNH^{2+}$ may not only be a metastable molecule, but also represents a thermochemically stable dication[10]). There exists, however, one ambiguity as far as this statement is concerned, which is related with the unknown thermochemistry of a *Coulomb* explosion into $FeN^+ + H^+$, the latter would be exothermic if $D(Fe^+-N)$ exceeds 95 kcal mol^{-1}. In fact, this perspective appears not unreasonable because the binding energy of the isolobal CH fragment to Fe^+ amounts to 101 kcal mol^{-1} [11]).

Interestingly, the $Fe^{2+}-NH$ binding energy is considerably higher compared to $D(Fe^{2+}-O) = 46$ kcal mol^{-1} or $D(Fe^{2+}-S) = 62$ kcal mol^{-1} [49]. This seems unexpected

---

[8]) Spin coupling is allowed concomitant with a spin change of the target gas. As the lowest-lying excitation of molecular oxygen ($^3\Sigma_g^- \rightarrow {}^1\Delta_g$) requires 0.98 eV, all processes involving spin changes at oxygen are higher in energy than the lowest possible excitation $FeNH^+$ ($^6\Sigma^+$) $\rightarrow FeNH^{2+}$ ($^5\Delta$) and cannot account for the experimental threshold energy.

[9]) This figure is derived as follows: The measured Q_{min} value is assigned to the vertical transition $FeNH^+$ ($^6\Sigma^+$) $\rightarrow FeNH^{2+}$ ($^5\Delta$), and corrected for the difference to the respective adiabatic process as well as for the energy gap to the $FeNH^{2+}$ ($^7\Sigma^-$) ground state, *i.e.*, $(16.3 \pm 0.4$ eV$) - 0.52$ eV $- 0.03$ eV $= 15.7 \pm 0.5$ eV.

[10]) For other examples of thermochemically stable di- and trications, see [47].

[11]) Further, at least for those metals M for which any data are available, $D(M^+-CH)$ and $D(M^+-N)$ are quite similar, *e.g.*, 96 *vs.* 89 kcal mol^{-1} for M = Sc, and 114 *vs.* 116 kcal mol^{-1} for M = Ti [48].

at first sight, because the binding energy of singly charged Fe^+-O exceeds that of Fe^+-NH by more than 10 kcal mol^{-1}, and $D(Fe^+-S)$ [49] is similar to $D(Fe^+-NH)$. We attribute the reversed order of binding energies for the dications to the presence of the additional H-atom in $FeNH^{2+}$, which facilitates the dispersion of the positive charges and increases the distance between the formal point charges. The *Mulliken* analysis gives partial charges of 1.53 (Fe), −0.09 (N), and 0.56 (H) for $FeNH^{2+}$ ($^7\Sigma^-$); the partial charges at Fe and H are separated by 3.14 Å. In contrast, FeS^{2+} ($^3\Delta$) has partial charges of 1.13 (Fe) and 0.87 (S) which are separated by 2.4 Å. Thus, the fact that $FeNH^{2+}$ is much more prone to *Coulomb* explosion than $FeNH^{2+}$ is nicely reflected by the simple *Mulliken* charge analysis [49]. In analogy, the fact that $IE(FeOH^+) = 17.0$ eV [50] is somewhat lower than $IE(FeO^+) = 17.7$ eV [49] may be rationalized by the presence of the additional proton.

Chemical Reactivity of FeNH+. The reactions of $FeNH^+$ with ethylene and benzene have been reported earlier by *Freiser* and coworkers [13], who observed C–N coupling products for both substrates. Encouraged by this important observation, we probed the versatility of $FeNH^+$ as an imine-transferring agent in the gas phase by reacting $FeNH^+$ with some selected inorganic and organic substrates. It should be pointed out that more than one spin state of $FeNH^+$ might be involved in all reactions mentioned below, due to the easy accessibility of at least two low-lying electronic states (see above). Following this line of reasoning, the observed rate constants might represent a superposition of rates for the individual spin states. However, a deconvolution of data to the individual spin contributions is not feasible at the present stage and beyond the scope of this study. All absolute rate constants are summarized in *Table 2*.

Table 2. *Absolute Rate Constants* k [10^{-10} cm^3 $molecules^{-1}$ s^{-1}] *and Efficiencies,* ϕ*, for the Reactions of* $FeNH^+$ *with Organic and Inorganic Substrates*[a])

Substrate	k	$\phi = k/k_C$	Substrate	k	$\phi = k/k_C$
Oxygen	0.04	0.007	Butane	6.6	0.55
Hydrogen	0.08	0.005	Isobutane	9.0	0.75
Methane	0.02	0.002	Benzene	8.7	0.70
Ethane	4.8	0.45	Toluene	13	1.0
Propane	5.7	0.50			

[a]) All rate constants are determined with an experimental error of ± 50%.

Water and Ammonia. Along with our studies concerning the generation of the $FeNH^+$ cation, the reactions with H_2O and NH_3 were studied. In addition to the slow reaction of $FeNH^+$ with H_2O to yield FeO^+ (see above), the only significant channels observed were the association products $(H_3N)FeO^+$ and $(H_3N)FeNH^+$[12]). Slow formation of Fe^+, $FeNH_2^+$, and $FeOH^+$ was also observed, but their amounts varied

[12]) For both ions, consecutive isomerizations to $HNFe(OH_2)^+$, $(H_2N)FeOH^+$, and $H_2NFeNH_2^+$ are likely to occur. As techniques like CID or ligand exchange render only information about the energetic order of exit channels rather than about the structural connectivity, the isomerization problem was not investigated any further.

from day to day. Corresponding blank experiments reveal, however, that these products arise either from residual reagents used in the generation of $FeNH^+$, *e.g.*, NH_3 and HN_3, or from hydrocarbons present as background impurities in the vacuum system.

Molecular Oxygen. The reaction of $FeNH^+$ with O_2 is featured by a low efficiency ($\phi = 0.007$) and affords Fe^+ and $FeOH^+$ as ionic products (*Reaction 8*). The presence of $Fe^{18}OH^+$ as ionic product in the reaction of $FeNH^+$ and $^{18}O_2$ excludes that the slow *Reaction 8b* arises from background contaminants rather than from an activation of O_2.

$$FeNH^+ + O_2 \longrightarrow \begin{cases} Fe^+ + HNO_2 & 75\% \quad (8a) \\ FeOH^+ + NO & 25\% \quad (8b) \end{cases}$$

The formation of both ionic products in *Reaction 8* requires the activation of the O–O bond in the course of the reaction. The O–O bond cleavage as well as N–O coupling can be described in terms of a metathesis mechanism, followed by reductive elimination (*Reaction 8a*) or H-migration and NO loss (*Reaction 8b*). Although the neutral products cannot be detected directly, thermochemical data predict that the formation of nitrous acid in *Reaction 8a* is much more exergonic than that of NO + OH, for example[13]). However, a detailed theoretical analysis of a related system has demonstrated that the mechanistic course of metal-mediated O_2 activations can be rather complex [51]. As Fe^+ is regenerated during the reaction, a catalytic protocol for the oxidation of NH_3 to HNO_2 involving the elementary *Reactions 5*, *2a*, and *8a* is conceivable[14]). Further studies may elucidate whether gas-phase experiments might contribute to clarify the mechanism of N–O coupling mediated by transition metals[15]).

Molecular Hydrogen. The reaction of $FeNH^+$ with H_2 yields atomic Fe^+ as the exclusive ionic product; NH_3 is, on thermochemical grounds, the only conceivable neutral species formed concomitantly (*Reaction 9*).

$$FeNH^+ + H_2 \longrightarrow Fe^+ + NH_3 \qquad 100\% \qquad (9)$$

In spite of the considerable exothermicity ($\Delta H_R = -33 \pm 2$ kcal mol^{-1}), the reaction efficiency is rather low ($\phi = 0.005$); accordingly, only about one in 200 collisions leads to the products. Moreover, although direct H–H bond activation must be involved, the reaction is associated with a surprisingly small kinetic isotope effect $KIE = \phi(H_2)/\phi(D_2) = 1.4 \pm 0.3$. Both features as well as the relative energies of the different $FeNH^+$ spin states are analogous to the FeO^+/H_2 system [34][42]. In the latter, the experimentally observed low efficiency and *KIE* led to the development of the TSR concept [35], which postulates that a spin crossover from the high-spin sextet to the low-spin quartet potential-energy surface is rate-determining. In fact, the systems $FeNH^+/H_2$ and FeO^+/H_2 are quite similar with respect to the reaction efficiencies

---

13) Thermochemical data predict the reaction $HNO_2 \rightarrow NO + OH$ to be endergonic by 40 kcal mol^{-1} ($\Delta H =$ 50 kcal mol^{-1}; 298 K $\cdot \Delta S = 10$ kcal mol^{-1}).

14) For other examples of catalytic processes under FTICR conditions, see [42][51][52].

15) For related examples of N–O bond cleavage in cationic metal complexes, see [53] and ref. cit. therein.

(0.005 *vs.* 0.006) as well as the isotope effects (1.4 *vs.* 1.3). Thus, we may qualitatively adopt the potential-energy surfaces outlined in theoretical studies of the FeO^+/H_2 system [34][54] also for the reaction of $FeNH^+$ with H_2. For a deeper understanding, however, a detailed theoretical analysis of the $FeNH^+/H_2$ system with special emphasis on the relative heights of barriers and crossing points of both spin surfaces is desirable (see below).

Methane. As already mentioned in the thermochemical section, $FeNH^+$ is capable to activate CH_4 to afford Fe^+ concomitant with neutral CH_3NH_2 (*Reaction 7*). Surprisingly, however, the reaction efficiency is quite low ($\phi = 0.002$), and also the associated *KIE* is small ($k(CH_4)/k(CD_4) = 1.3 \pm 0.4$). These results are in marked contrast to the related FeO^+/CH_4 system [55][56]. Further, $FeNH^+$ activates CH_4 less efficiently than H_2 ($\phi(H_2)/\phi(CH_4) = 2.5$), whereas a reversed order is observed for FeO^+ ($\phi(H_2)/\phi(CH_4) = 0.08$) [34a]. Qualitatively, X-transfers (X = O, NH) from FeX^+ to H_2 and CH_4, respectively, are influenced by two opposing factors: *i*) From a thermochemical point of view, the reactions with H_2 are favored due to the much larger reaction exothermicities; *i.e.*, $\Delta_R H$ amounts to -117 and -101 kcal mol^{-1}, respectively, for $H_2 + X \rightarrow H_2X$ (X = O, NH), whereas bond insertion to CH_4 according to $CH_4 + X \rightarrow CH_3XH$ is much less exothermic (-90 and -78 kcal mol^{-1}, respectively). *ii*) Kinetically, however, the higher polarizability and the higher density of states of CH_4 deepen the well and, thus, increase the lifetimes of the respective encounter complexes. The striking dissimilarity between the $FeNH^+/H_2$ *vs.* FeO^+/H_2 and the $FeNH^+/CH_4$ *vs.* FeO^+/CH_4 couples requests for a concise conceptual rationalization. At present, the only glance for a possible explanation we can provide is that recent *ab initio* studies of FeO^+/H_2 and FeO^+/CH_4 indicate that the barrier for activation of H_2 is smaller than for CH_4 [54][56] relative to the respective encounter complexes [$FeO^+ \cdot RH$] on the sextet surfaces; the barriers along the quartet surfaces amount to 16 kcal mol^{-1} for R = H compared to 22 kcal mol^{-1} for $R = CH_3$. This difference may be attributed to the energy demand for achieving a five-coordinated C-atom en route to the activation of CH_4. Assuming that the relative energies for minima and transition structures are similar for the $FeNH^+/H_2$ and $FeNH^+/CH_4$ systems, the barrier heights might rationalize the observed reaction rates. As already mentioned above, a precise theoretical analysis of the reaction coordinate, including the detailed role of electron spin, seems indispensable for a satisfying understanding of the experimental findings. Such an effort is certainly close to the limits of currently available theoretical methods; however, the distinct experimental borderlines provided in this study render this comparison a challenging, but very attractive benchmark for computational studies on C–H bond activation by bare transition metals.

Another difference of the $FeNH^+/CH_4$ and FeO^+/CH_4 systems concerns the abstraction of an H$^\bullet$ radical from CH_4 which leads to $FeOH^+$ as a major product of the FeO^+/CH_4 couple; in contrast the analogous $FeNH_2^+$ fragment could not be observed in significant amounts in the $FeNH^+/CH_4$ system. However, the kinetic restrictions associated with an H$^\bullet$ abstraction are not expected to be higher than those of *Reaction 7*. Instead, the differences in product distributions may in part be attributed to simple thermochemistry, because H$^\bullet$ abstraction from CH_4 to afford $FeNH_2^+$ is predicted to be endothermic by 2 ± 4 kcal mol^{-1}, while the analogous reaction of FeO^+

to yield $FeOH^+$ is apparently exothermic (-2 ± 3 kcal mol^{-1}). Although slightly endothermic reactions can occur under the experimental conditions (*Reaction 2a* is reversible, for example), they might be suppressed as soon as more favorable competitive pathways exist. Nevertheless, it has been pointed out previously [34a] that the branching between the Fe^+/CH_3XH and $FeXH^+/CH_3^{\bullet}$ channels (X = O, NH) may be influenced by rather subtle effects and is not fully understood.

Ethane. Compared to the activation of H_2 and CH_4 by $FeNH^+$, that of C_2H_6 is much more efficient ($\phi = 0.45$) and involves three different channels (*Reaction 10*).

$$FeNH^+ + C_2H_6 \longrightarrow \begin{cases} Fe^+ + [C_2,H_7,N] & 10\% & (10a) \\ Fe(C_2H_4)^+ + NH_3 & 30\% & (10b) \\ Fe(NH_3)^+ + C_2H_4 & 60\% & (10c) \end{cases}$$

The enhanced efficiency can be attributed to the larger polarizability and the weaker C–H bond strength in C_2H_6, as well as the availability of additional reaction channels. The mechanism leading to the generation of $Fe^+ + [C_2,H_7,N]$ is probably similar for $FeNH^+/CH_4$ and $FeNH^+/C_2H_6$, but the latter system is *ca.* 30 times more efficient. The reaction products coincide nicely with those obtained from the FeO^+/C_2H_6 couple, where Fe^+ (10%), $Fe(C_2H_4)^+$ (70%), and $Fe(H_2O)^+$ (20%) are generated [57], and we assume a similar reaction mechanism (*Scheme 1*). For example, the ratio of Fe^+ *vs.* $Fe(L)^+$ formation agrees within experimental error for C_2H_6 reacting with either FeO^+ or $FeNH^+$. The different product ratios of the C_2H_4/H_2O losses for FeO^+ *vs.* the C_2H_4/NH_3 eliminations for $FeNH^+$ simply reflect the differences in the metal–ligand binding energies, which decrease in the order $D(Fe^+-NH_3) > D(Fe^+-C_2H_4) > D(Fe^+-H_2O)$[16]).

Scheme 1

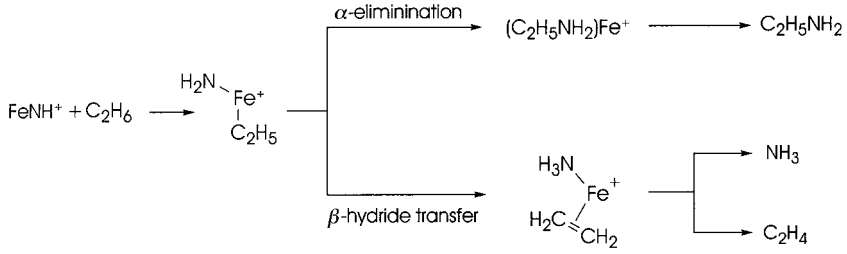

Propane. The higher homolog C_3H_8 behaves very similarly, and bond activation by $FeNH^+$ occurs with a reaction efficiency of $\phi = 0.50$ (*Reaction 11*).

---

16) $BDE(Fe-C_2H_4)^+ \approx 30-35$ kcal mol^{-1} and $BDE(Fe-H_2O)^+ \approx 28-33$ kcal mol^{-1} are taken from [48]. $BDE(Fe^+-NH_3) = 43.9$ kcal mol^{-1} is taken from [58].

$$FeNH^+ + C_3H_8 \rightarrow \begin{cases} Fe^+ + [C_3,H_9,N] & 5\% & (11a) \\ Fe(C_3H_6)^+ + NH_3 & 25\% & (11b) \\ Fe(NH_3)^+ + C_3H_6 & 65\% & (11c) \\ [Fe,C,H_5,N]^+ + C_2H_4 & 5\% & (11d) \end{cases}$$

When $FeNH^+$ is reacted with [2,2-D_2]propane, the ionic products Fe^+, $Fe(NH_2D)^+$, $Fe(C_3H_5D)^+$, and $[Fe,C,H_5,N]^+$ are formed. The generation of $[C_3,H_9,N]$, NH_3, and C_3H_8 as neutral products can be explained with a sequence analogous to the one shown in *Scheme 1*, involving insertion into a primary or secondary C–H bond as the first step. In contrast, *Reaction 11d* cannot arise from insertion into a secondary C–H bond, but implies an activation of the primary C–H bond and a subsequent β-methyl shift according to *Scheme 2*. This scenario is further supported by the labeling experiment with [2,2-D_2]propane, where only $[Fe,C,H_5,N]^+$ and neutral $C_2H_2D_2$ are formed in the channel corresponding to *Reaction 11d*. The most probable structures of $[Fe,C,H_5,N]^+$ have previously been characterized as *i*) $Fe(CH_3NH_2)^+$, a genuine Fe^+ complex of CH_3NH_2, and *ii*) $H_3C-Fe^+-NH_2$, the corresponding insertion species [59]. For the elucidation of further mechanistic details, it is instructive to compare the present results with previous studies on systems closely related to the $FeNH^+/C_3H_8$ couple. For example, in analogy to *Reactions 11b–11d*, bare Fe^+ reacts with $C_3H_7NH_2$ to afford neutral NH_3 and propene as minor (3% and 17%), respectively, and C_2H_4 as major (63%) products [60], and a very similar product distribution is observed in the unimolecular dissociation of $Fe^+/C_3H_7NH_2$ complexes, *i.e.*, losses of neutral NH_3, (4%), C_2H_4 (55%), and C_3H_6 (19%), respectively [61]. Formation of bare Fe^+ in analogy to *Reaction 11a* can, of course, not be monitored for the $Fe^+/C_3H_7NH_2$ couple and also does not occur in the metastable ion dissociation of $Fe^+/C_3H_7NH_2$ complexes. Metastable ion dissociation of a Fe^+/i-$PrNH_2$ complex, formed in a chemical ionization source, yields an almost exclusive loss of H_2 (99%) next to a minor loss of CH_4 (1%). When the reaction of Fe^+ with i-$PrNH_2$ is carried out in an ICR spectrometer, NH_3 (5%), C_3H_6 (10%), H_2 (55%), and CH_4 (10%) are the main neutral fragments lost [62]. In contrast, dehydrogenation is not observed at all for the $FeNH^+/C_3H_8$ couple. As mentioned above, $FeNH^+$ is assumed to react with C_3H_8 *via* C–H bond activation to yield $H_2N-Fe^+-C_3H_7$, because an alternative initial C–C bond activation would generate the same intermediate that is proposed as the starting point for all products observed for the $Fe^+/C_3H_7NH_2$ couple. As the $FeNH^+/C_3H_8$ couple is higher in energy ($\Delta H_f(FeNH^+ + C_3H_8) = 277$ kcal mol^{-1}) compared to $Fe^+ + C_3H_7NH_2$ ($\Delta H_f = 265$ kcal mol^{-1}) or Fe^+ + i-$PrNH_2$ ($\Delta H_f = 261$ kcal mol^{-1}), the marked differences in the product distributions cannot be traced back to thermochemical reasons. They must be rather ascribed to different initial structures that are not equilibrated due to the existence of

Scheme 2

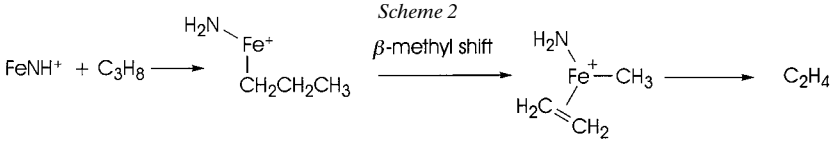

significant kinetic barriers. The following kinetic restrictions seem to prevail: *i*) The different products generated from $FeNH^+/C_3H_8$ and $Fe^+/C_3H_7NH_2$ show that the $H_2N-Fe^+-R \rightleftarrows Fe^+-NH_2R$ equilibration is much slower than the rates for product formation. *ii*) A previous study has shown that the β-methyl shift depicted in *Scheme 2* is reversible [59]. However, the $FeNH^+/H_3CCD_2CH_3$ couple produces only $Fe(C_3H_5D)^+$ and no $Fe(C_3H_6)^+$ or $Fe(C_3H_4D_2)^+$; this finding demonstrates that the $(C_2H_4)Fe^+(CH_3)(NH_2) \rightleftarrows (C_3H_7)-Fe^+-NH_2$ interconversion is again slow compared to the β-hydride elimination. These bottlenecks also prevent a determination of the ratio of primary *vs.* secondary C–H bond activation for the $FeNH^+/C_3H_8$ couple.

The reactions of the analogous FeO^+/C_3H_8 system are quite similar to those of the iron imine; the major difference is that loss of a $CH_3^{\bullet}$ radical leading to $(C_2H_4)FeOH^+$ instead of expulsion of C_2H_4 is observed. Similar to the CH_4 case, a pathway involving only losses of closed-shell neutrals is followed by $FeNH^+/C_3H_8$, whereas a radical reaction is favored for FeO^+/C_3H_8.

Butane. From $FeNH^+$ and C_4H_{10}, only two ionic products are formed with a reaction effeciency of $\phi = 0.55$. Preservation of the C_4 skeleton in both pathways suggests that no C–C activation takes place in this system (*Reaction 12*).

$$FeNH^+ + C_4H_{10} \longrightarrow \begin{cases} Fe(NH_3)^+ + C_4H_8 & 65\% \quad (12a) \\ Fe(C_4H_6)^+ + NH_3 + H_2 & 35\% \quad (12b) \end{cases}$$

Notwithstanding the simple product distribution, a rather complex mechanistic scheme has to be considered, because two principal problems were encountered. *i*) In contrast to the smaller alkanes, the formation of Fe^+ is hardly observed ($< 2\%$). Although Fe^+ reacts efficiently with C_4H_{10}, we exclude that the absence of Fe^+ can be traced back to consecutive reactions, as continuous double resonance ejection of Fe^+ does not affect the product distribution. Besides, none of the primary products of the Fe^+/C_4H_{10} couple, *i.e.*, $Fe(C_2H_4)^+$, $Fe(C_3H_6)^+$, and $Fe(C_4H_8)^+$, are present in quantities larger than 1%. However, C–H bond insertion of $FeNH^+$ cannot be slower for C_4H_{10} than for C_2H_6 or C_3H_8, because this would affect all products derived from this branching point. Instead, we attribute the lack of generating bare Fe^+ in *Reaction 12* to the efficient competition of β-hydride transfer in the case of C_4H_{10}. *ii*) While *Reaction 12a* parallels the formation of $Fe(NH_3)^+$ in the reactions of $FeNH^+$ with C_2H_6 and C_3H_8, respectively, the second channel involves loss of NH_3 concomitant with dehydrogenation to afford $Fe(C_4H_6)^+$. The product ratio $Fe(NH_3)^+/Fe(C_4H_6)^+$ 65 : 35 conflicts with the Fe^+ affinities of the ligands in that the binding energy of C_4H_6 (presumably buta-1,3-diene) to Fe^+ exceeds that of NH_3 to Fe^+ (48 kcal mol^{-1} *vs.* 43.9 kcal mol^{-1})[17]) [58][63]. Thus, the final ionic products are probably not formed *via* a common intermediate such as $(H_3N)Fe^+(C_4H_6)$. Hence, we suggest a mechanistic scenario (*Scheme 3*) which involves formation of the insertion species **1** in the first step[18]) followed by β-hydrogen transfer to afford the bisligated complex **2**. For the

---

[17]) Another value is $D(Fe^+-C_4H_6) = 43.4 \pm 2.4$ kcal mol^{-1}, see [64].

[18]) We cannot quantify the ratio of primary *vs.* secondary bond activation. For the sake of simplicity, only secondary bond activation is shown in *Scheme 3*.

latter, loss of the butene ligand is more facile than that of NH_3, *i.e.*, $D(Fe^+-C_4H_8) = 39$ kcal mol^{-1} *vs.* $D(Fe^+-NH_3) = 43.9$ kcal mol^{-1}, and thus accounting for the predominance of *Reaction 12a*. If NH_3 is lost from **2**, the intermediate butene complex undergoes rapid dehydrogenation to afford Fe^+/butadiene. The fact that Fe^+/butene is not observed at all in the experiment may be attributed to the fact that formation of $Fe(C_4H_8)^+ + NH_3$ from the $FeNH^+/C_4H_{10}$ couple is by *ca.* 44 kcal mol^{-1} exothermic such that this intermediate is assumed to be 'hot' giving rise to rapid consecutive dehydrogenation.

Scheme 3

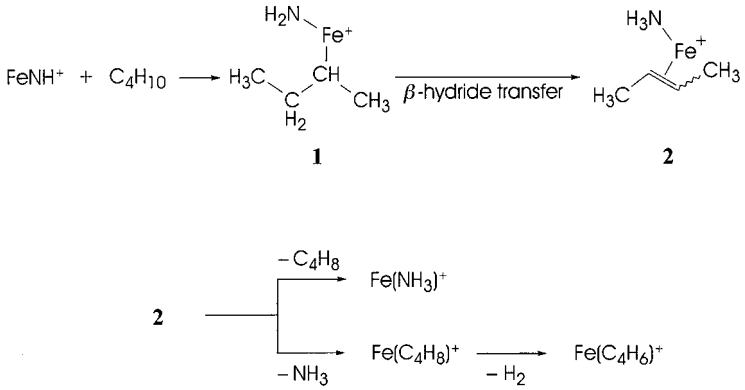

Isobutane. In remarkable distinction from the linear C_4H_{10} isomer, five different pathways are followed by the $FeNH^+$/isobutane couple (*Reaction 13*; $\phi = 0.75$).

$$FeNH^+ + \text{i-}C_4H_{10} \rightarrow \begin{cases} Fe^+ + [C_4,H_{11},N] & 15\% & (13a) \\ Fe(C_4H_8)^+ + NH_3 & 25\% & (13b) \\ Fe(NH_3)^+ + C_4H_8 & 45\% & (13c) \\ Fe(CH_3NH_2)^+ + C_3H_6 & 10\% & (13d) \\ Fe(C_3H_8N)^+ + CH_3^{\cdot} & 5\% & (13e) \end{cases}$$

In fact, the reaction channels observed with isobutane resemble those of the $FeNH^+/C_3H_8$ couple rather than those found for C_4H_{10}. Thus, *i*) reductive elimination (*Reaction 13a*) is observed, *ii*) losses of NH_3 and butene (*Reactions 13b* and *13c*) compete with each other, and their ratio agrees with the corresponding Fe^+ affinities, *i.e.*, $D(Fe^+-\text{isobutane}) = 39$ kcal mol^{-1} [64] *vs.* $D(Fe^+-NH_3) = 43.9$ kcal mol^{-1}, and *iii*) *Reaction 13d* follows the mechanistic scheme outlined for loss of C_2H_4 in the $FeNH^+/C_3H_8$ case. In contrast to $FeNH^+/C_3H_8$, however, the activated CH_3 group is partly lost (*Reaction 13e*), but the total amount of radical products is still much lower compared to FeO^+/isobutane where loss of a $CH_3^{\cdot}$ radical accounts for 65% of the products. Double dehydrogenation to afford $Fe(C_4H_6)^+$ is not observed at all, which agrees perfectly with the formation of an isobutene/Fe^+ complex in *Reaction 13b*.

Before concluding the section about aliphatic substrates, we would like to discuss briefly the formation of Fe^+ in the reactions with C_2H_6, C_3H_8, and isobutane in some more detail. As the neutral by-products concomitant with Fe^+ cannot be characterized directly in the ICR experiment, all thermochemically accessible structures have to be taken into account. Next to the formation of an alkylamine *via* α-elimination, the generation of two neutrals, *i.e.*, alkene and NH_3, by a twofold ligand loss from the (alkene)$Fe^+(NH_3)$ intermediate is also possible (*Scheme 1*). In fact, although the production of alkylamine is by 11–14 kcal mol^{-1} more exothermic than that of the alkene and NH_3, the free enthalpy of both exit channels is similar due to entropic contributions. However, two arguments suggest that C–N coupling to yield the alkylamine actually takes place. *i*) The generation of Fe^+ from the $FeNH^+/CH_4$ reaction must coincide with C–N bond coupling, as all neutral products other than CH_3NH_2 are much higher in energy. *ii*) According to earlier studies [61], the barrier between (alkene)$Fe(NH_3)^+$ and Fe^+ + alkylamine is *lower* than the Fe^+ + alkylamine exit channel. Moreover, the $FeNH^+$/alkane entrance channel is 12–16 kcal mol^{-1} higher in energy than the Fe^+ + alkylamine exit channel. Therefore, the generation of Fe^+ + alkylamine from the $FeNH^+$/alkane couple cannot be prevented by a kinetic barrier or by a thermochemical restriction. In other words, the pathway $FeNH^+$ + alkane $\rightarrow$ Fe^+ + alkylamine is feasible in principle, and there is no reason why the reaction should not occur. In summary, the formation of Fe^+ and alkylamine in the reactions of $FeNH^+$ with C_2H_6, C_3H_8, and isobutane is very likely to occur, although it cannot be excluded that Fe^+ partially arises from an alternative pathway involving twofold ligand loss.

Benzene. NH-Group transfer from $FeNH^+$ to benzene (C_6H_6) to afford ionized aniline has been reported by *Freiser* and coworkers [13]. In addition to this channel, two other minor pathways are also observed which were not mentioned previously (*Reaction 14*; $\phi = 0.70$).

$$\text{FeNH}^+ + \text{C}_6\text{H}_6 \rightarrow \begin{cases} \text{Fe}^+ + \text{C}_6\text{H}_5\text{NH}_2 & 10\% \quad (14a) \\ \text{C}_6\text{H}_5\text{NH}_2^{+\bullet} + \text{Fe} & 80\% \quad (14b) \\ \text{Fe}(\text{C}_5\text{H}_6)^+ + \text{HCN} & 10\% \quad (14c) \end{cases}$$

Formation of atomic iron in *Reactions 14a* and *14b* corresponds to a transfer of the imine unit to benzene, and, on thermochemical grounds, only $C_6H_5NH_2$ appears as a conceivable structure of the organic counterpart[19]). Formation of aniline in *Reactions 14a* and *14b* is further supported by the fact that the major pathway leads to a positively charged organic product, rather than a metal cation. The preference for *Reaction 14b* follows nicely the ordering of the ionization energies, *i.e.*, $IE(Fe) = 7.87$ eV and $IE(C_6H_5NH_2) = 7.72$ eV. As far as the reaction mechanism is concerned, the occurrence of *Reaction 14c* and the negligible kinetic isotope effect observed for C_6D_6 ($k(C_6H_6)/k(C_6D_6) = 1.2$) imply close similarities to the FeO^+/C_6H_6 system[20]).

---

[19]) For more recent synthetic procedures for the amination of arenes, see [65].

[20]) The reaction of FeO^+ with C_6H_6 yields $Fe^+ + C_6H_5OH$ (56%), $Fe(C_5H_6)^+ + CO$, (37%), $Fe(C_5H_5)^+ +$ [H,C,O] (2%), and $Fe(C_6H_4)^+ + H_2O$ (5%) [66].

Toluene. The reaction of $FeNH^+$ with toluene occurs at the collision limit ($\phi = 1.0$). Loss of molecular hydrogen is by far the dominant reaction channel next to some minor pathways (*Reaction 15*).

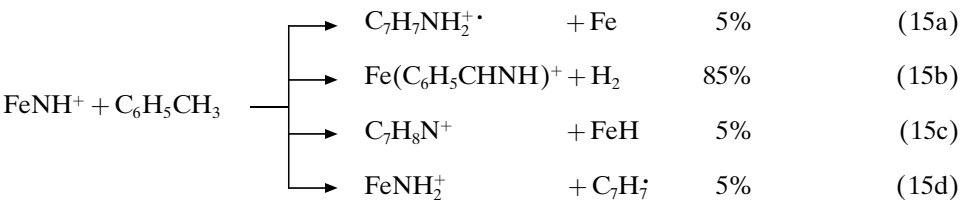

Labeling experiments reveal that the dehydrogenation pathway (*Reaction 15b*) does not involve ring positions, because only H_2 is lost from $C_6D_5CH_3$. Therefore, we can exclude a $-CH_2C_6H_4NH-$ chelate complex to iron. When $FeNH^+$ is reacted with $C_6H_5CD_3$, almost equal amounts of HD and D_2 losses but no expulsion of H_2 are observed, which indicates that an exchange of H-atoms between the imine unit and the benzylic positions is feasible. Moreover, the ratio between the corresponding ionic products formed, *i.e.*, $Fe(C_6H_5CHDN)^+$ and $Fe(C_6H_5CD_2N)^+$, is shifted in favor of the former with increasing reaction times due to exchange with background protons. An exchange of the last D-atom in $Fe(C_6H_5CHDN)^+$ is not observed, however. On the basis of these findings, a benzylideneamine unit bound to iron is suggested as the structure of the product ion, *i.e.*, $C_6H_5CH{=}NH/Fe^+$. Hydride transfer to yield neutral FeH (*Reaction 15c*) involves the benzylic C–H bond as demonstrated by the exclusive formation of neutral FeD from the $C_6H_5CD_3/FeNH^+$ couple. The organic radical cation formed in *Reaction 15a* is assigned to toluidine rather than to $C_6H_5CH_2NH_2$ based on the respective ionization energies. The fact that the positive charge is located on the organic part is indicative for formation of toluidine (*IE*s = 7.24–7.50 eV), because, for $C_6H_5CH_2NH_2$ (*IE* = 8.64 eV), the positive charge is expected to remain on iron (*IE* = 7.87 eV) [41]. However, due to their low intensities, a further characterization of the products formed in *Reactions 15a* and *15c* was not possible.

The $FeNH^+/C_6H_5CH_3$ couple resembles the $FeO^+/C_6H_5CH_3$ analog [67] as far as the remarkable regioselectivity is concerned. Although both $FeNH^+$ and FeO^+ are also able to activate aromatic positions, side-chain attack is strongly favored. However, the main pathway of the $FeO^+/C_6H_5CH_3$ reaction is due to carbocation formation, *i.e.*, $C_7H_7^+ + FeOH$ (86%), while a reaction yielding H_2 elimination is preferred for $FeNH^+$. Finally, we note in passing that similar fast processes like H_2 elimination or NH transfer were observed for xylenes and mesitylene. These efficient reactions thereby prevent a reliable determination of *IE*(FeNH) using the bracketing approach (see above).

Conclusion. – Summarizing the reactivity of $FeNH^+$ towards all investigated substrates, three central features emerge:

1) $FeNH^+$ possesses an intrinsically high reactivity and is able to activate a broad range of substrates. The activation of 'inert' species like molecular oxygen or methane is also feasible, but inefficient due to the operation of kinetic barriers.

2) Many reactivity patterns of $FeNH^+$ match those of FeO^+, but the reaction efficiencies are somewhat lower and radical processes are disfavored for $FeNH^+$.

3) For most organic substrates, at least partial C–N bond coupling is accomplished.

The $FeNH^+$ cation provides a model system for the examination of transition-metal-mediated imine transfer in the gas phase. Its spectroscopical and chemical properties were studied by means of theoretical calculations and mass-spectrometric experiments. Probably the most attractive chemical feature of $FeNH^+$ is its ability to transfer an imine unit to a wide range of substrates by C–N and N–O bond formation. Currently, the extension of this concept to other transition metals is being investigated, especially to group 4–7 metals that proved to be valuable for imine chemistry in the condensed phase.

Mechanistically, the reactions of $FeNH^+$ with hydrocarbons display many similarities to those of FeO^+. Yet some remarkable differences described in the present study will require a detailed theoretical analysis of the mechanistic course of oxygen *vs.* imine transfer in the gas phase.

We are grateful to the *Deutsche Forschungsgemeinschaft*, the *Fonds der Chemischen Industrie*, and the *Volkswagen-Stiftung* for financial support. *M.B.* and *I.K.* acknowledge the *Stiftung Stipendien-Fonds des Verbandes der Chemischen Industrie* for Ph. D. scholarships. We thank Dr. *H. Hugl*, *Bayer AG*, Leverkusen, for having brought this topic to our attention.

REFERENCES

[1] a) R. C. Larock, 'Comprehensive Organic Transformations', VCH Publishers, New York, 1989; b) 'Houben-Weyl, Methoden der organischen Chemie', Band 11, Ed. E. Müller, Thieme Verlag, Stuttgart, 1957.
[2] 'Gmelin Handbook of Inorganic and Organometallic Chemistry', Nitrogen, Supplement B1, 8th edn., Springer-Verlag, Berlin, 1993.
[3] Ref. 1 and 2 in M. H. Schofield, T. P. Kee, J. T. Anhaus, R. R. Schrock, K. H. Johnson, W. M. Davis, *Inorg. Chem.* **1991**, *30*, 3595.
[4] a) T. I. Gountchev, T. D. Tilley, *J. Am. Chem. Soc*. **1997**, *119*, 12831; b) D. S. Glueck, J. Wu, F. J. Hollander, R. G. Bergman, *ibid*. **1991**, *113*, 2041; c) E. A. Maata, R. A. D. Wentworth, *Inorg. Chem.* **1979**, *18*, 2409.
[5] a) B. A. Arndtsen, H. F. Sleiman, L. McElwee-White, *Organometallics* **1993**, *12*, 2440; b) B. A. Arndtsen, H. F. Sleiman, A. K. Chang, L. McElwee-White, *J. Am. Chem. Soc*. **1991**, *113*, 4871.
[6] S. M. Rocklage, R. R. Schrock, *J. Am. Chem. Soc*. **1980**, *102*, 7808.
[7] a) J. Du Bois, C. S. Tomooka, J. Hong, E. M. Carreira, *Acc. Chem. Res.* **1997**, *30*, 364; b) J. T. Groves, T. Takahashi, *J. Am. Chem. Soc*. **1983**, *105*, 2073.
[8] P. J. Walsh, A. M. Baranger, R. G. Bergman, *J. Am. Chem. Soc*. **1992**, *114*, 1708.
[9] a) D. F. Schafer II, P. T. Wolczanski, *J. Am. Chem. Soc*. **1998**, *120*, 4881; b) C. P. Schaller, C. C. Cummins, P. T. Wolczanski, *ibid*. **1996**, *118*, 591; c) C. C. Cummins, S. M. Baxter, P. T. Wolczanski, *ibid*. **1988**, *110*, 8731; d) P. J. Walsh, F. J. Hollander, R. G. Bergmann, *ibid*. **1988**, *110*, 8729.
[10] a) K. A. Jorgensen, *Inorg. Chem.* **1993**, *32*, 1521; b) T. R. Cundari, *J. Am. Chem. Soc.* **1992**, *114*, 7879; c) W. A. Nugent, R. J. McKinney, R. V. Kasowski, F. A. Van-Catledge, *Inorg. Chim. Acta* **1982**, *65*, L91.
[11] a) D. E. Clemmer, L. S. Sunderlin, P. B. Armentrout, *J. Phys. Chem.* **1990**, *94*, 3008; b) D. E. Clemmer, L. S. Sunderlin, P. B. Armentrout, *J. Phys. Chem.* **1990**, *94*, 208.
[12] K. K. Irikura, J. L. Beauchamp, *J. Am. Chem. Soc*. **1989**, *111*, 75.
[13] S. W. Buckner, J. R. Gord, B. S. Freiser, *J. Am. Chem. Soc*. **1988**, *110*, 6606.
[14] D. R. A. Ranatunga, Y. D. Hill, B. S. Freiser, *Organometallics* **1996**, *15*, 1242.
[15] T.-C. Lau, Z. Wu, J. Wang, K. W. M. Sin, R. Guevremont, *Inorg. Chem.* **1996**, *35*, 2169.
[16] D. Schröder, H. Schwarz, *Angew. Chem., Int. Ed. Engl*. **1995**, *34*, 1973.
[17] D. E. Clemmer, P. B. Armentrout, *J. Phys. Chem.* **1991**, *95*, 3084.
[18] a) K. Eller, W. Zummack, H. Schwarz, *J. Am. Chem. Soc.* **1990**, *112*, 621; b) K. Eller, H. Schwarz, *Int. J. Mass Spectrom. Ion Processes* **1989**, *93*, 243.
[19] A. G. Marshall, C. L. Hendrickson, G. S. Jackson, *Mass Spectrom. Rev.* **1998**, *17*, 1.
[20] R. A. Forbes, F. H. Laukien, J. Wronka, *Int. J. Mass Spectrom. Ion Processes* **1988**, *83*, 23.
[21] a) R. Srinivas, D. Sülzle, T. Weiske, H. Schwarz, *Int. J. Mass Spectrom. Ion Processes* **1991**, *107*, 369; b) R. Srinivas, D. Sülzle, W. Koch, C. H. DePuy, H. Schwarz, *J. Am. Chem. Soc***. 1991**, *113*, 5970.

[22] P. Dai, S. McCullough-Catalano, M. Bolton, A. D. Jones, C. B. Lebrilla, *Int. J. Mass Spectrom. Ion Processes* **1995**, *144*, 67.
[23] K. Lammertsma, P. v. R. Schleyer, H. Schwarz, *Angew. Chem., Int. Ed. Engl.* **1989**, *28*, 1321.
[24] R. Steudel, P. W. Schenk, 'Handbuch der präparativen anorganischen Chemie', Ed. G. Brauer, F. Enke Verlag, Stuttgart, 1975, p. 455.
[25] a) P. J. Stephens, F. J. Devlin, C. F. Chabalowski, M. J. Frisch, *J. Phys. Chem.* **1994**, *98*, 11623; b) A. D. Becke, *J. Chem. Phys.* **1993**, *98*, 5648.
[26] Gaussian 94, Revision E.1, M. J. Frisch, G. W. Trucks, H. B. Schlegel, P. M. W. Gill, B. G. Johnson, M. A. Robb, J. R. Cheeseman, T. Keith, G. A. Petersson, J. A. Montgomery, K. Raghavachari, M. A. Al-Laham, V. G. Zakrzewski, J. V. Ortiz, J. B. Foresman, C. Y. Peng, P. Y. Ayala, W. Chen, M. W. Wong, J. L. Andres, E. S. Replogle, R. Gomperts, R. L. Martin, D. L. Fox, J. S. Binkley, D. J. Defrees, J. Baker, J. P. Stewart, M. Head-Gordon, C. Gonzalez, J. A. Pople, Gaussian, Inc., Pittsburg PA, 1995.
[27] MOLPRO 96, H.-J. Werner and P. J. Knowles (Eds.); J. Almlöf, R. D. Amos, M. J. O. Deegan, S. T. Elbert, C. Hampel, W. Meyer, K. Peterson, R. Pitzer, A. J. Stone, P. R. Taylor, R. Lindh.
[28] H. J. Werner, P. J. Knowles, *Theor. Chim. Acta* **1990**, *78*, 175.
[29] P.-O. Widmark, P.-Å. Malmqvist, B. O. Roos, *Theor. Chim. Acta* **1990**, *77*, 291.
[30] P.-O. Widmark, B. J. Persson, B. O. Roos, *Theor. Chim. Acta* **1991**, *79*, 419.
[31] S. K. Loh, E. R. Fisher, L. Lian, R. H. Schultz, P. B. Armentrout, *J. Phys. Chem.* **1989**, *93*, 3159.
[32] K. Eller, H. Schwarz, *Inorg. Chem.* **1990**, *29*, 3250.
[33] a) T. Su, *J. Chem. Phys.* **1994**, *100*, 4703; b) *ibid.* **1988**, *89*, 5355; c) T. Su, W. Chesnavich, *ibid.* **1982**, *76*, 5183.
[34] a) D. Schröder, H. Schwarz, D. E. Clemmer, Y. Chen, P. B. Armentrout, V. I. Baranov, D. K. Böhme, *Int. J. Mass Spectrom. Ion Processes* **1997**, *161*, 175; b) V. I. Baranov, G. Javahery, A. C. Hopkinson, D. K. Böhme, *J. Am. Chem. Soc.* **1995**, *117*, 12801; c) D. Schröder, A. Fiedler, J. Schwarz, H. Schwarz, *Inorg. Chem.* **1994**, *33*, 5094; d) M. M. Kappes, R. H. Staley, *J. Am. Chem. Soc.* **1981**, *103*, 1286.
[35] a) S. Shaik, M. Filatov, D. Schröder, H. Schwarz, *Chem. Eur. J.* **1998**, *4*, 193; b) S. Shaik, D. Danovich, A. Fiedler, D. Schröder, H. Schwarz, *Helv. Chim. Acta* **1995**, *78*, 1393; c) A. Fiedler, D. Schröder, S. Shaik, H. Schwarz, *J. Am. Chem. Soc.* **1994**, *116*, 10734.
[36] A. Fiedler, J. Hrušák, W. Koch, H. Schwarz, *Chem. Phys. Lett.* **1993**, *211*, 242.
[37] D. G. Musaev, K. Morokuma, *J. Chem. Phys.* **1994**, *101*, 10697.
[38] A. Fiedler, S. Iwata, *Chem. Phys. Lett.* **1997**, *271*, 143.
[39] M. L. McKee, *J. Am. Chem. Soc.* **1990**, *112*, 2601.
[40] a) V. C. Gibson, E. L. Marshall, C. Redshaw, W. Clegg, M. R. J. Elsegood, *J. Chem. Soc.*, *Dalton Trans.* **1996**, 4197; b) J. T. Anhaus, T. P. Kee, M. H. Schofield, R. R. Schrock, *J. Am. Chem. Soc.* **1990**, *112*, 1642.
[41] a) S. G. Lias, J. F. Liebmann, J. L. Holmes, R. D. Levin, W. G. Mallard, *J. Phys. Chem. Ref. Data* **1988**, *17*, 695; b) C. E. Moore, 'Atomic Energy Levels', National Bureau of Standards, Washington D.C., 1949.
[42] D. Schröder, A. Fiedler, M. F. Ryan, H. Schwarz, *J. Phys. Chem.* **1994**, *98*, 68.
[43] G. Bouchoux, J. Y. Salpin, D. Leblanc, *Int. J. Mass Spectrom. Ion Processes* **1996**, *153*, 37.
[44] S. W. Buckner, B. S. Freiser, *Polyhedron* **1988**, *7*, 1583.
[45] R. H. Schultz, P. B. Armentrout, *Organometallics* **1992**, *11*, 828.
[46] a) C. A. Schalley, G. Hornung, D. Schröder, H. Schwarz, *Chem. Soc. Rev.* **1998**, *27*, 91; b) N. Goldberg, H. Schwarz, *Acc. Chem. Res.* **1994**, *27*, 347; c) F. Turecek, *Org. Mass Spectrom.* **1992**, *27*, 1087.
[47] a) D. Schröder, J. N. Harvey, H. Schwarz, *J. Phys. Chem. A* **1998**, *102*, 3639; b) D. Schröder, M. Diefenbach, T. Klapötke, H. Schwarz, *Angew. Chem., Int. Ed. Engl.*, in press.
[48] 'Organometallic Ion Chemistry', Ed. B. S. Freiser, Kluwer Academic Publishers, Dordrecht, 1996.
[49] J. N. Harvey, C. Heinemann, A. Fiedler, D. Schröder, H. Schwarz, *Chem. Eur. J.* **1996**, *2*, 1230.
[50] S. McCullough-Catalano, C. B. Lebrilla, *J. Am. Chem. Soc.* **1993**, *115*, 1441.
[51] M. Pavlov, M. R. A. Blomberg, P. E. M. Siegbahn, R. Wesendrup, C. Heinemann, H. Schwarz, *J. Phys. Chem. A* **1997**, *101*, 1567.
[52] a) D. Stöckigt, H. Schwarz, *Liebigs Ann. Chem.* **1995**, 429; b) R. Wesendrup, D. Schröder, H. Schwarz, *Angew. Chem.* **1994**, *106*, 1232; *ibid., Int. Ed. Engl.* **1994**, *33*, 1174; c) M. F. Ryan, D. Stöckigt, H. Schwarz, *J. Am. Chem. Soc.* **1994**, *116*, 9565; d) P. Schnabel, M. P. Iron, K. G. Weil, *J. Phys. Chem.* **1991**, *95*, 9688; e) D. Schröder, H. Schwarz, *Angew. Chem.* **1990**, *102*, 1468; *Angew. Chem. Int. Ed. Engl.* **1990**, *29*, 1433.
[53] D. Schröder, J. Müller, H. Schwarz, *Organometallics* **1993**, *12*, 1972.
[54] M. Filatov, S. Shaik, *J. Phys. Chem. A* **1998**, *102*, 3835.
[55] D. Schröder, A. Fiedler, J. Hrušák, H. Schwarz, *J. Am. Chem. Soc.* **1992**, *114*, 1215.

[56] a) K. Yoshizawa, Y. Shiota, T. Yamabe, *Organometallics* **1998**, *17*, 2825; b) K. Yoshizawa, Y. Shiota, T. Yamabe, *J. Am. Chem. Soc.* **1998**, *120*, 564; c) K. Yoshizawa, Y. Shiota, T. Yamabe, *Chem. Eur. J.* **1997**, *3*, 1160.
[57] D. Schröder, H. Schwarz, *Angew. Chem., Int. Ed. Engl.* **1990**, *29*, 1431.
[58] D. Walter, P. B. Armentrout, *J. Am. Chem. Soc.* **1998**, *120*, 3176.
[59] S. Karrass, D. Stöckigt, D. Schröder, H. Schwarz, *Organometallics* **1993**, *12*, 1449.
[60] S. J. Babinec, J. Allison, *J. Am. Chem. Soc.* **1984**, *10*, 7718.
[61] S. Karrass, T. Prüsse, K. Eller, H. Schwarz, *J. Am. Chem. Soc.* **1989**, *111*, 9018.
[62] M. Brönstrup, H. Schwarz, unpublished results.
[63] R. L. Hettich, T. C. Jackson, E. M. Stanko, B. S. Freiser, *J. Am. Chem. Soc.* **1986**, *108*, 5086.
[64] D. Schröder, H. Schwarz, *J. Organomet. Chem.* **1995**, *504*, 123.
[65] a) K. Hori, M. Mori, *J. Am. Chem. Soc.* **1998**, *120*, 7651; b) G. Wüllner, H. Jänsch, S. Kannenberg, F. Schubert, G. Boche, *Chem. Commun.* **1998**, 1509; c) J. F. Hartwig, *Angew. Chem.* **1998**, *110*, 2154; *Angew. Chem., Int. Ed. Engl.* **1998**, *37*, 2046.
[66] a) H. J. Becker, D. Schröder, W. Zummack, H. Schwarz, *J. Am. Chem. Soc.* **1994**, *116*, 1096; b) D. Schröder, H. Schwarz, *Helv. Chim. Acta* **1992**, *75*, 1281.
[67] D. Schröder, H. Florencio, W. Zummack, H. Schwarz, *Helv. Chim. Acta* **1992**, *75*, 1792.

Received October 9, 1998